THE JOURNAL OF NAVIGATION (2012), **65**, 15–28. © The Royal Institute of Navigation
doi:10.1017/S0373463311000518

Using Constraints for Shoe Mounted Indoor Pedestrian Navigation

Khairi Abdulrahim[1,2], Chris Hide[1], Terry Moore[1] and Chris Hill[1]

[1] *Nottingham Geospatial Institute (NGI), Nottingham, UK.*
[2] *Faculty of Science and Technology, Universiti Sains Islam Malaysia (USIM), Malaysia.*
(E-mail: isxka3@nottingham.ac.uk)

Shoe mounted Inertial Measurement Units (IMU) are often used for indoor pedestrian navigation systems. The presence of a zero velocity condition during the stance phase enables Zero Velocity Updates (ZUPT) to be applied regularly every time the user takes a step. Most of the velocity and attitude errors can be estimated using ZUPTs. However, good heading estimation for such a system remains a challenge. This is due to the poor observability of heading error for a low cost Micro-Electro-Mechanical (MEMS) IMU, even with the use of ZUPTs in a Kalman filter. In this paper, the same approach is adopted where a MEMS IMU is mounted on a shoe, but with additional constraints applied. The three constraints proposed herein are used to generate measurement updates for a Kalman filter, known as 'Heading Update', 'Zero Integrated Heading Rate Update' and 'Height Update'.

The first constraint involves restricting heading drift in a typical building where the user is walking. Due to the fact that typical buildings are rectangular in shape, an assumption is made that most walking in this environment is constrained to only follow one of the four main headings of the building. A second constraint is further used to restrict heading drift during a non-walking situation. This is carried out because the first constraint cannot be applied when the user is stationary. Finally, the third constraint is applied to limit the error growth in height. An assumption is made that the height changes in indoor buildings are only caused when the user walks up and down a staircase. Several trials were shown to demonstrate the effectiveness of integrating these constraints for indoor pedestrian navigation. The results show that an average return position error of 4·62 meters is obtained for an average distance of 1557 meters using only a low cost MEMS IMU.

KEY WORDS

1. Inertial Measurement Units (IMU). 2. Zero Integrated Heading Rate (ZIHR)
3. Zero Integrated Heading Rate (ZIHR).

1. INTRODUCTION. Navigating in GPS denied environments such as urban canyons and indoors using GPS technology is often very difficult (Lachapelle, 2004). This is due to the absence of direct line of sight to GPS satellites to acquire GPS signals. As a result, the quality of the received signal (if it can be received) deteriorates largely due to multipath or weakened signal power. Although High Sensitivity GPS (HSGPS) receivers can be used to detect weak signals, often the signal is not reliable

enough to produce an accurate position solution. An example was demonstrated (Odijk and Kleijer, 2007, 2008) where the use of HSGPS produced corrupted solutions in an indoor environment due to weak and reflected signals.

Resorting to different types of navigation technology that do not use Radio Frequency (RF) signals is therefore a potential alternative. Inertial sensors satisfy this criterion because they do not receive or transmit any signals. Furthermore, the advent of low cost MEMS inertial sensors suits the requirement for low cost consumer applications such as pedestrian navigation. MEMS Inertial Measurement Units (IMU) normally consist of accelerometers and gyros that produce measurements (acceleration and attitude rate) in a body coordinate frame. Attitude parameters are then used to transform these measurements into a desired frame such as the navigation frame and from these, one can work out the position of the system. However, due to its low cost nature, it is prone to errors (Pang and Liu, 2001; Godha, 2006; Park and Gao, 2006) that eventually cause large position errors.

One idea to reduce the solution error is to strap the IMU on a user's foot or shoe to perform Zero Velocity Updates (ZUPT) (Jiemenez et al., 2009; Skog et al., 2010; Hide et al., 2009; Foxlin, 2005). Due to the strap-down configuration, it has the advantage of measuring the foot's velocity directly. It is therefore valid to assume that during the stance phase (zero velocity) of a walking gait, the IMU should produce zero velocity measurements for the foot's velocity. In practise however, this is not entirely true because of the inherent errors of the inertial sensors. Therefore, the non-zero velocity measurement from the strapped-down IMU during this period is considered as an error, and can be subsequently corrected. For example, this can be performed by feeding back this error to a control system. Furthermore, if this measurement update is used in an estimation filter such as Kalman filter, it can not only be used to correct the user's walking velocity, but also help restrict the position and attitude errors, and estimate the sensor bias errors. This is because the Kalman filter uses an inertial error model that builds up information on the correlation between the states modelled such as position, velocity, attitude and sensor biases. A 15-state Kalman filter estimating position, velocity, attitude, gyro bias and accelerometer bias errors is used for the work in this paper as described in Abdulrahim et al. (2011).

Nonetheless, heading drift is still a major concern in low-cost-self-contained-IMU systems, even with the use of ZUPT measurements. Although frequent use of ZUPTs consistently bounds many IMU errors, optimal estimation of heading becomes a difficult process because there is no direct correlation between velocity and heading (Godha and Lachapelle, 2008). Therefore there is a need to have other measurement updates that have high correlation with heading angle to aid the estimation process.

In Abdulrahim et al. (2011), we presented an approach of using heading aiding using very basic information derived from maps or aerial images. This alleviates the need for detailed room-level maps of the inside of buildings which are typically unavailable, particularly for private buildings. The heading measurements are able to maintain accurate heading without the need for any additional sensors such as magnetometers. This paper describes the developed algorithm that constrains a walk in a typical building to only walking in cardinal headings. It is shown to consistently and effectively restrict heading drift for all test datasets, resulting in a significant improvement in an INS-only positioning.

This paper describes further developments to the indoor positioning algorithm. An additional measurement is applied to address the problem of heading drift when the

user is stationary since the cardinal heading algorithm is only applicable when the user is moving. The measurement is termed Zero Integrated Heading Rate (ZIHR) (Shin, 2005) where knowledge of previous and current heading rates are used to constrain the drift. To the authors' knowledge, ZIHR has never been used before in pedestrian navigation to constrain heading drift during prolonged stop. Most of the results in the literature demonstrate walking without stopping in an extended period of time, which is slightly unusual for pedestrians. Another measurement is also introduced to restrict vertical position drift when the pedestrian is inside buildings.

Trials have taken place at the University of Nottingham using a low cost MEMS inertial sensor to show the effectiveness of combining the constraints. This paper demonstrates that using the constraints described, average position error is consistently kept below 5 meters while walking for an average distance of approximately 1·5 kilometres. To conclude, this paper presents an effective approach to restrict heading drift and vertical drift using constraints in a typical low cost indoor pedestrian navigation system. The improvement made in estimating heading error with the use of this approach will be analysed. It is envisaged that self-contained inertial navigation could be made possible in a longer duration, at least in typical indoor environments.

2. HEADING CONSTRAINT DURING WALKING.

This section describes the algorithm developed (Abdulrahim et al., 2010, 2011) where a measurement is derived to constrain heading drift as a pedestrian walks around a building. The underlying idea is that when a pedestrian walks through a building, most of their motion is constrained to one of four principle (termed cardinal) directions. This is due to the simple construction of most buildings which are typically rectangular in shape and have the rooms and corridors aligned with the outer walls. The orientation of the building can be derived from maps or aerial images and a database can be constructed that can be used to aid navigation. For this work, it is helpful to highlight that building orientation will be consistent with the Course Over Ground (COG) direction that the user walks as opposed to heading or yaw which is the true orientation of the x-axis of the IMU with respect to North.

The algorithm makes two important assumptions. Firstly, it is assumed that the pedestrian will typically (but not always) walk in a direction that is consistent with the orientation of the outer walls of the building. Secondly, it is assumed that the difference between the COG (calculated from the difference in position of two steps) and the outer orientation of the building is the result of heading drift plus some uncertainty due to the pedestrian not walking in a straight line. This second assumption is only valid because there is a large acceleration caused by the foot moving through a step. Because there is a large acceleration, the heading error is observable through the position difference since heading is used to determine the orientation of the accelerometer axes. For other applications such as vehicle navigation, it is not possible to use this assumption since the vehicle may be travelling at constant velocity and therefore heading has no effect on position.

The algorithm can be described using Figure 1. The COG is computed using $a\tan 2\left(\frac{dE}{dN}\right)$ where dN and dE are the change in position in North and East axes respectively caused by a step being made between epochs k and $k+1$. To remove steps

https://doi.org/10.1017/S0373463311000518 Published online by Cambridge University Press

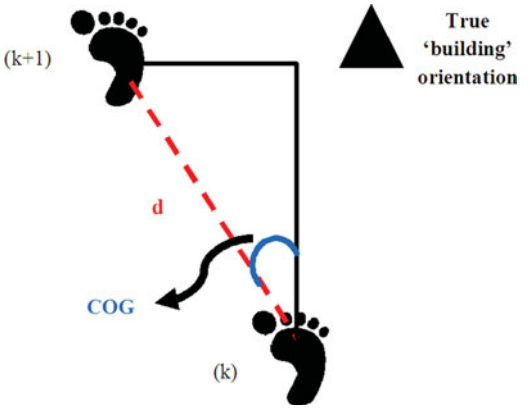

Figure 1. Illustration of the heading measurement at each epoch.

that are not consistent with the building orientation we introduce the condition,

$$C_1 = \begin{cases} 1, & COG \leqslant t_{COGmax} \\ 0, & otherwise \end{cases} \tag{1}$$

where t_{COGmax} is an empirically derived threshold that is used to exclude steps that are not consistent with the building such as when walking around corners or not walking straight along a corridor. The threshold has to be large enough to accommodate the heading drift of the IMU as well as small variations in COG that are caused by the pedestrian not walking exactly in straight lines.

A second condition is also used,

$$C_2 = \begin{cases} 1, & t_{dmin} \leqslant d \leqslant t_{dmax} \\ 0, & otherwise \end{cases} \tag{2}$$

where $d = [dN^2 + dE^2]^{0.5}$ is the footstep length. This threshold is used to ensure that only steps of a typical stride length are used to compute COG. If both C_1 and C_2 return true (logical 1), then a measurement is added to the Kalman filter, otherwise, no update is sent to the Kalman filter.

The measurement used for the Kalman filter is the difference between the COG calculated from the change in position between steps and the orientation of the building. A measurement update is applied by forming the observation,

$$\delta\varphi = \left[\frac{\delta\varphi}{\delta\phi_N} \quad \frac{\delta\varphi}{\delta\phi_E} \quad \frac{\delta\varphi}{\delta\phi_D} \right] \boldsymbol{\phi} + n_k \tag{3}$$

where n_k is the measurement noise with covariance $R_k = E(n_k n_k^T)$ which is large enough to accommodate steps that are not consistent with the building (which is closely related to the value used for t_{COGmax}); the partial derivatives are formed with respect to $\boldsymbol{\phi}$ which is a vector of attitude errors in the navigation frame as modelled in the Kalman filter. See (Shin, 2005) for details including derivation of the partial derivatives) and,

$$\delta\varphi = \varphi_{building} - COG \tag{4}$$

where, $\delta\varphi$ is the IMU heading error and $\varphi_{building}$ is the current 'building' orientation.

https://doi.org/10.1017/S0373463311000518 Published online by Cambridge University Press

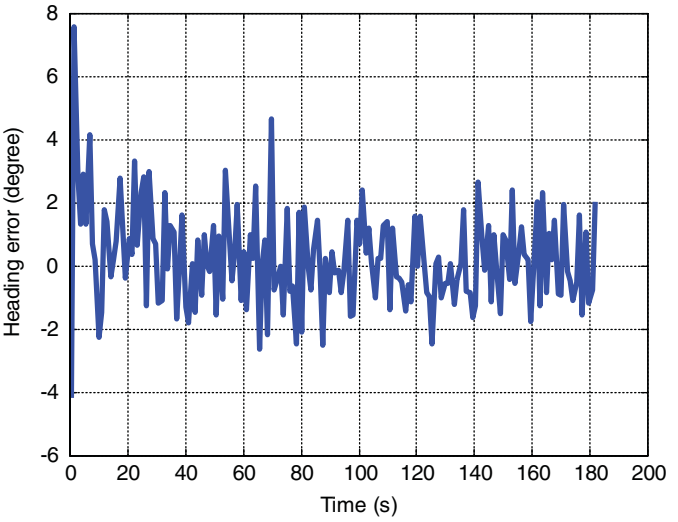

Figure 2. Heading error for walking in a straight walk.

The heading measurement is tested by walking along a straight line (next to a straight road). Figure 2 shows the values for $\delta\varphi$ that are used in the Kalman filter. The values comprise the Inertial Navigation System (INS) heading error, other small INS drift, and also the variations of the user's step in relation to the true COG. A Microstrain 3DM-GX3 inertial sensor is used with the accelerometer bias stability quoted as ±0·01 g, and for the 300 degree/s model, the gyro biases are specified as ±0·2 degree/s. The particular IMU used has a limit of 1200 degree/s for angular rotation and 18 *g* for acceleration. The standard deviation of heading difference is only 1·54° while the maximum heading difference is 7·58° (which corresponds to the 10° threshold used).

Figure 3 shows the position error after approximately 3 minutes of walking in a straight line. The blue line represents the position error using the heading algorithm while the black line represents position error without using the algorithm. Using the heading update, the final North position error is 1·25 m whereas the end position error is 49·77 m if the algorithm is not used. Further results in more realistic situations are described towards the end of this paper.

3. HEADING CONSTRAINT DURING STOP. In this paper, an approach proposed (Shin, 2005) to constrain heading drift for a wheeled vehicle when it stops is adopted for our pedestrian navigation system. This is because during a stationary condition, roll and pitch errors can be constrained by applying ZUPTs, but not the heading error due to its poor observability. The algorithm is known as Zero Integrated Heading Rate (ZIHR) and it uses the knowledge of previous and current heading rate to stop the accumulation of heading drift error. The measurement equation is written as follows:

$$\frac{\varphi_k - \varphi_{k-1}}{\Delta t_k} \approx \begin{bmatrix} 0 & \sec\theta \sin\phi & \sec\theta \cos\phi \end{bmatrix} \boldsymbol{b}_g + n_k \tag{5}$$

https://doi.org/10.1017/S0373463311000518 Published online by Cambridge University Press

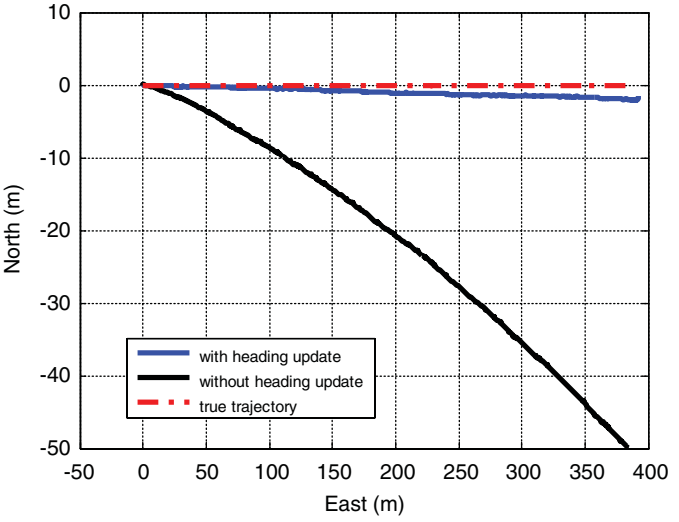

Figure 3. Position with and without heading update.

where φ_k is the INS heading; roll (ϕ) and pitch (θ) are considered as constants over the time interval Δt_k; $\boldsymbol{b}_g$ is the vector of body frame gyro biases; n_k is the remaining noise term; and k is the epoch. Due to the term sec θ, ZIHR cannot be applied when pitch is close to ±90°. For this algorithm, the epochs k and $k+1$ correspond to times either side of a step.

Before the ZIHR measurement model can be used in the Kalman filter, we introduce two conditions that need to be satisfied. First, a zero velocity condition is checked to ensure that the system is stationary (i.e. the pedestrian has stopped walking). If this event returns true, a second check is performed by checking whether the foot is rotating or not. This is important to highlight a case when the pedestrian stops walking and rotates his foot at the same time. The conditions can be written as:

$$C_3 = \begin{cases} 1, & |\boldsymbol{V}_k| \leqslant t_{\boldsymbol{V}max} \\ 0, & otherwise \end{cases} \tag{6}$$

$$C_4 = \begin{cases} 1, & |\boldsymbol{\omega}_k| \leqslant t_{\boldsymbol{\omega}max} \\ 0, & otherwise \end{cases} \tag{7}$$

where $\boldsymbol{V}_k$ is the three dimensional velocity of the IMU and $\boldsymbol{\omega}_k$ is the three dimensional rotation determined by the gyros. The logical "1"s in equations (6) and (7) mark the detected stance phase (ZUPT event) and non-rotating foot respectively. If both C_3 and C_4 return true (logical 1), then the ZIHR measurement model is used to update attitude in the Kalman filter, otherwise, no update is sent to the Kalman filter. The threshold $t_{\boldsymbol{\omega}max}$ must be set to be larger than the expected total gyro bias and yet small enough to ensure the IMU is not physically rotating.

A static test is first conducted to illustrate the result of using the ZIHR measurement using the Microstrain 3DM-GX3 sensor used in the previous test. The IMU is put on a stationary table for 16 minutes and is initialised with a known position and attitude to

https://doi.org/10.1017/S0373463311000518 Published online by Cambridge University Press

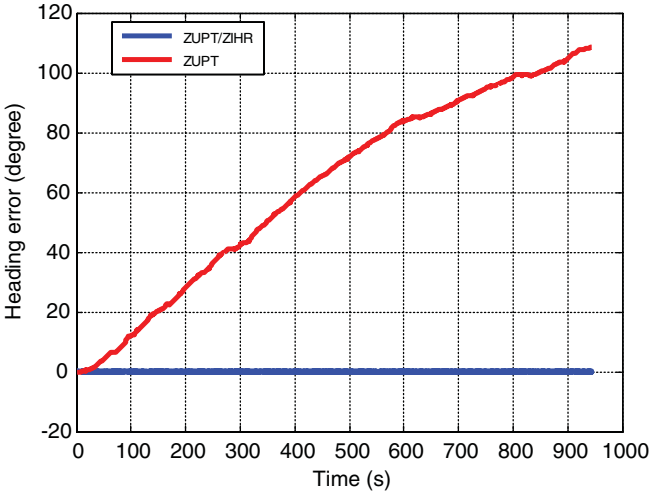

Figure 4. Heading errors during static test for ZUPT and ZUPT/ZIHR.

represent a condition where pedestrian stops walking for a long period. A comparison is made between using ZUPT only (normal approach) and using ZUPT with ZIHR applied. Figure 4 shows the heading solution and it clearly shows that the heading drifts quite considerably if only ZUPT is used. After 60 seconds a heading error of 5° is observed, which then grows to about 100° after 900 seconds. When the ZIHR constraint is applied, an accuracy of better than 0·04° is achieved.

An alternative to using ZIHR is to fix the heading whenever conditions C_3 and C_4 are true. However, this would not make full use of the measurement as achieved using ZIHR where full correlation between states is exploited. Alternatively a yaw measurement can be applied using Equation 3 where $\delta\varphi$ is computed as the difference between the current yaw and the yaw estimate before conditions C_3 and C_4 are true. However, if a heading measurement is used directly, it will result in an over optimistic estimate of the uncertainty of the attitude states. Consider an example where initial heading uncertainty and heading measurement noise are set to 10° and 1° respectively. Figure 5 shows the standard deviation of the down axis attitude error state, $\boldsymbol{\phi}_D$. Here we see that the standard deviation for the yaw measurement case drops to a small value which is unrealistic as the measurement is not a true measurement (such as from an external sensor). Instead we are only wishing to stop the heading error increasing and we wish to preserve the covariance in the Kalman filter. Thus, ZIHR is able to make full use of the measurement while preserving the covariance in the Kalman filter.

4. HEIGHT CONSTRAINT. A height measurement is also introduced for our pedestrian navigation system to restrict the IMU height drift in indoor environments. Without the availability of height measurements from sensors such as GPS, the height of the INS solution will drift to some extent due to accumulation of errors in the inertial sensors that are not fully removed through ZUPT measurements.

https://doi.org/10.1017/S0373463311000518 Published online by Cambridge University Press

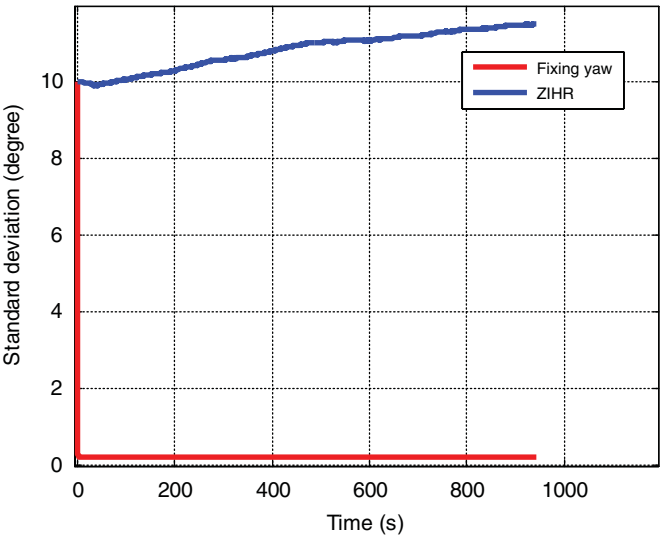

Figure 5. Down attitude error standard deviation for ZIHR and Heading Constraint.

Therefore, we make use of the knowledge that in most indoor environments, the floor will be level, and we assume that changes in height in indoor environment would only be caused by walking up or down the staircases. Since it is reasonable to assume that a pedestrian's foot lies on the floor during every stance phase of walking event, we create a predetermined height threshold that represents steps height, to limit the height error growth that gets updated in every stance phase. A change in height over one step is calculated and if it is below the threshold, the height from previous epoch calculation is maintained and projected to the next epoch. Thus, a fifth condition (C_5) is used:

$$C_5 = \begin{cases} 1, & |\delta h| \leqslant t_{hstep} \\ 0, & otherwise \end{cases} \tag{8}$$

where $|\delta h| = |h_k - h_{k-1}|$ (where epochs k and $k-1$ correspond to different steps) with empirical threshold, $t_{hstep} = 0{\cdot}05$ m. If both C_3 and C_5 return true (logical 1), then height at the last epoch is preserved to update the position state vector in the Kalman filter, otherwise no update is applied. Using the measurement in this way unfortunately results in an over optimistic covariance of the height due to the issues discussed in regard to yaw measurements in the previous section. Although not strictly rigorous, the benefits of applying the height correction indoors are thought to outweigh any issues caused by an overoptimistic height covariance estimate. A measurement update is applied by forming the observation:

$$\delta h = \begin{bmatrix} 0 & 0 & -1 \end{bmatrix} \delta p + n_k \tag{9}$$

where δp is the IMU position error state vector with measurement noise n_k.

A height constraint test is carried out by walking down and up a staircase. A pedestrian walked from the top to the bottom of the stairs, then walked up

https://doi.org/10.1017/S0373463311000518 Published online by Cambridge University Press

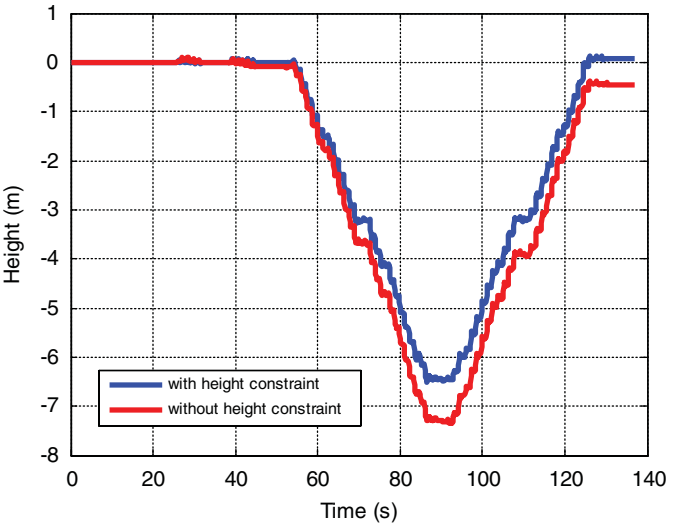

Figure 6. IMU height output with and without height constraint.

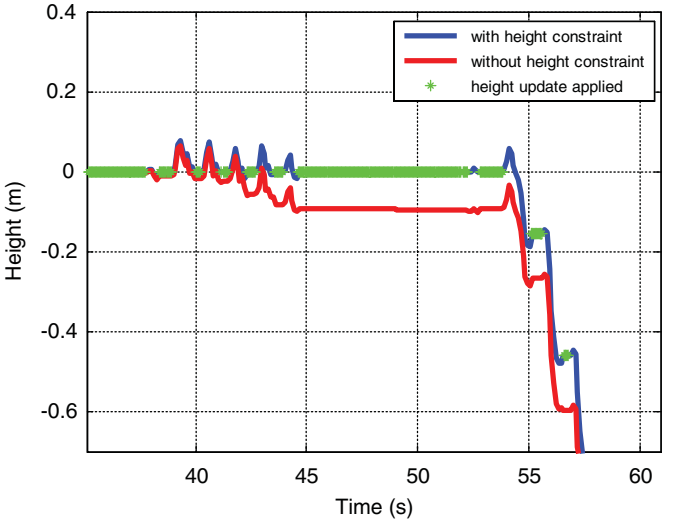

Figure 7. Height constraint is being updated.

again and stopped at the same starting position. The stairs consist of 42 steps with ±16·5 cm each in height (measured using steel tape and assumed to be the truth), totalling 6·93 m in height. Figure 6 shows the INS height, with and without height constraint, and Figure 7 shows the period when the height constraint was performed.

From Figure 6, when height constraint is used, the end position error for this trial is 6·6 cm, and it correctly identified 42 steps. In contrast, without height constraint,

https://doi.org/10.1017/S0373463311000518 Published online by Cambridge University Press

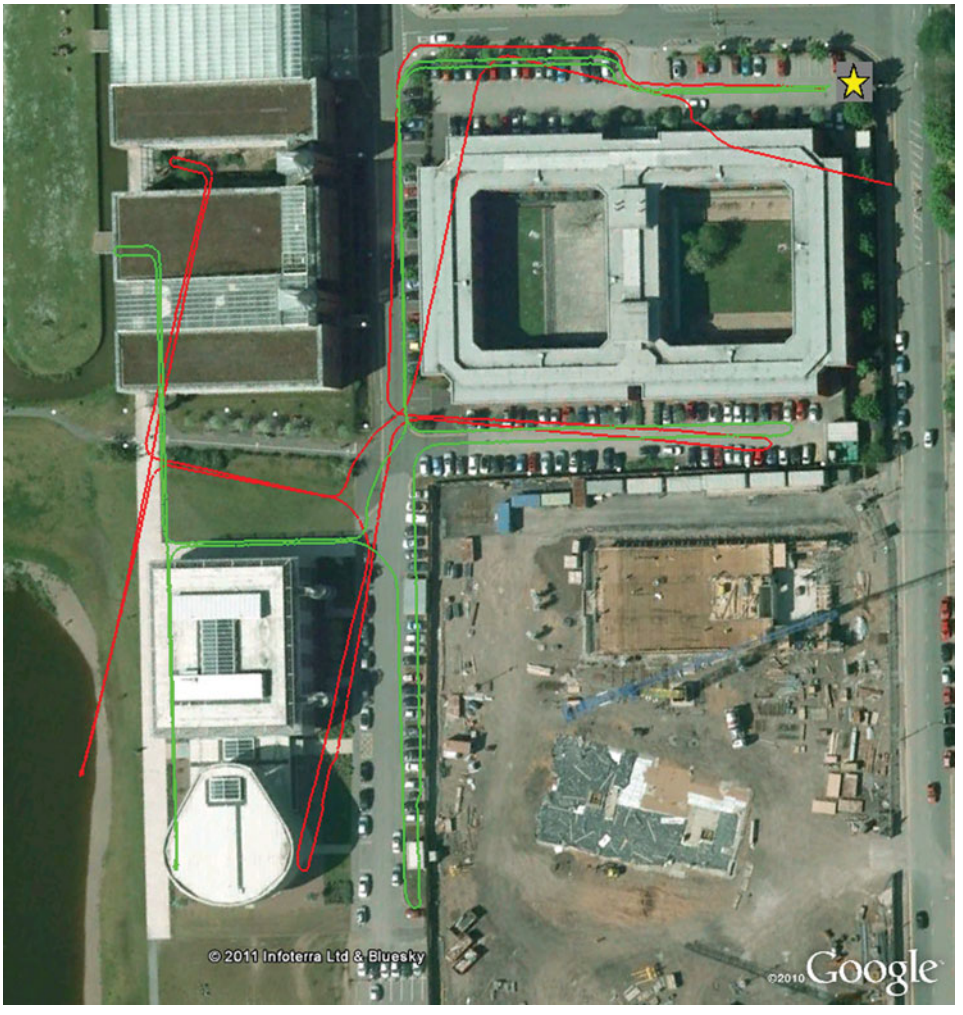

Figure 8. Example of position output from Trial 8.

the end position error has drifted to 45 cm. The start of the data in Figure 6 is further magnified and shown in Figure 7. It clearly shows that when height constraint is performed (green marker), height error does not grow as opposed to when height constraint is not used (red plot). However it is important to highlight that for height constraint to hold true, changes in height in indoor buildings are assumed to be caused by staircases. Therefore, the height constraint will not work as expected if we consider other situations where the height change between epochs might not be as big, such as when walking on a ramp on the floor.

5. FULL TRIALS. Several field trials have been conducted in Nottingham, UK. The IMU used was a Microstrain 3DM-GX3 as described earlier in this paper. Table 1 summarises the output of the walks. 'Return Height Error' represents the

https://doi.org/10.1017/S0373463311000518 Published online by Cambridge University Press

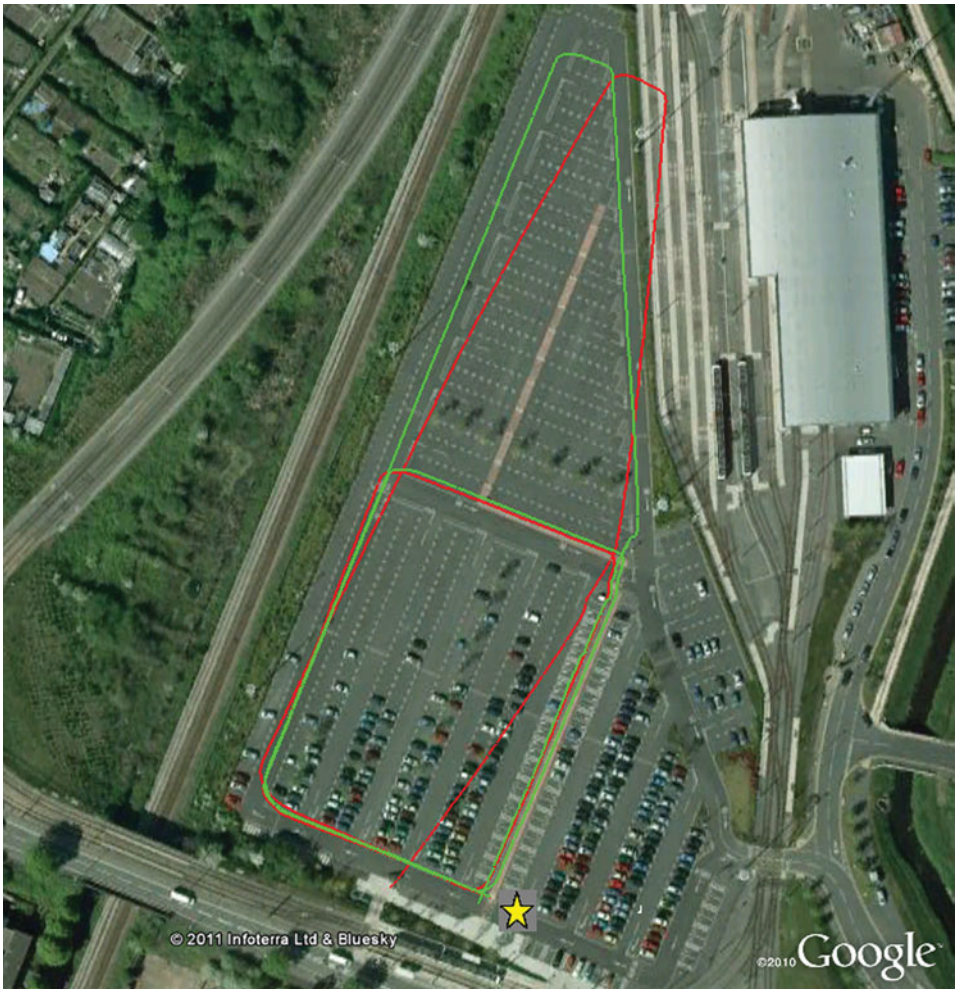

Figure 9. Example of position output from Trial 8.

difference in height while 'Return Position Error' represents the difference in position, after returning to the same location. The 'Constraint' column consists of results that use all the proposed constraints, while the 'No Constraint' column represents results that use only ZUPT as measurement update. From these eight field trials that use proposed constraints, it was found that for an average duration of 23·79 minutes and an average total distance travelled of 1557 m, the average return height error is 0·39 m, and the average return position error is 4·62 m. In contrast, trials that do not use the proposed constraints have an average error in height and position error of 40·38 m and 153·62 m respectively. Figures 8, 9 and 10 show the visualisation of three outputs from Table 1 trials, where heading drift errors have been reduced significantly. In the Figures, the yellow star marks the start and end of the walking trials, the red line marks the position output without using constraints and the green line shows the position output when constraints are applied.

https://doi.org/10.1017/S0373463311000518 Published online by Cambridge University Press

Table 1. Comparison of errors for proposed system with and without constraints applied.

Trial	Duration (minutes)	Distance (m)	Return Height Error		Return Position Error	
			Constraints (m)	No constraints (m)	Constraints (m)	No constraints (m)
1	15·7	496·8	~ 0·00	5·58	6·25	270·42
2	12·7	902·8	~ 0·00	0·32	3·96	28·63
3	40·0	3000·0	~ 0·00	71·46	4·42	34·58
4	30·4	1973·7	0·98	16·21	4·23	109·6
5	21·9	1443·9	0·15	0·75	7·60	518·24
6	38·8	2665·3	~ 0·00	26·34	3·11	204·21
7	16·0	918·8	0·20	85·08	6·20	38·73
8	14·8	1058·4	0·23	117·35	1·19	24·52
AVERAGE	23·8	1557·5	0·39	40·39	4·62	153·62

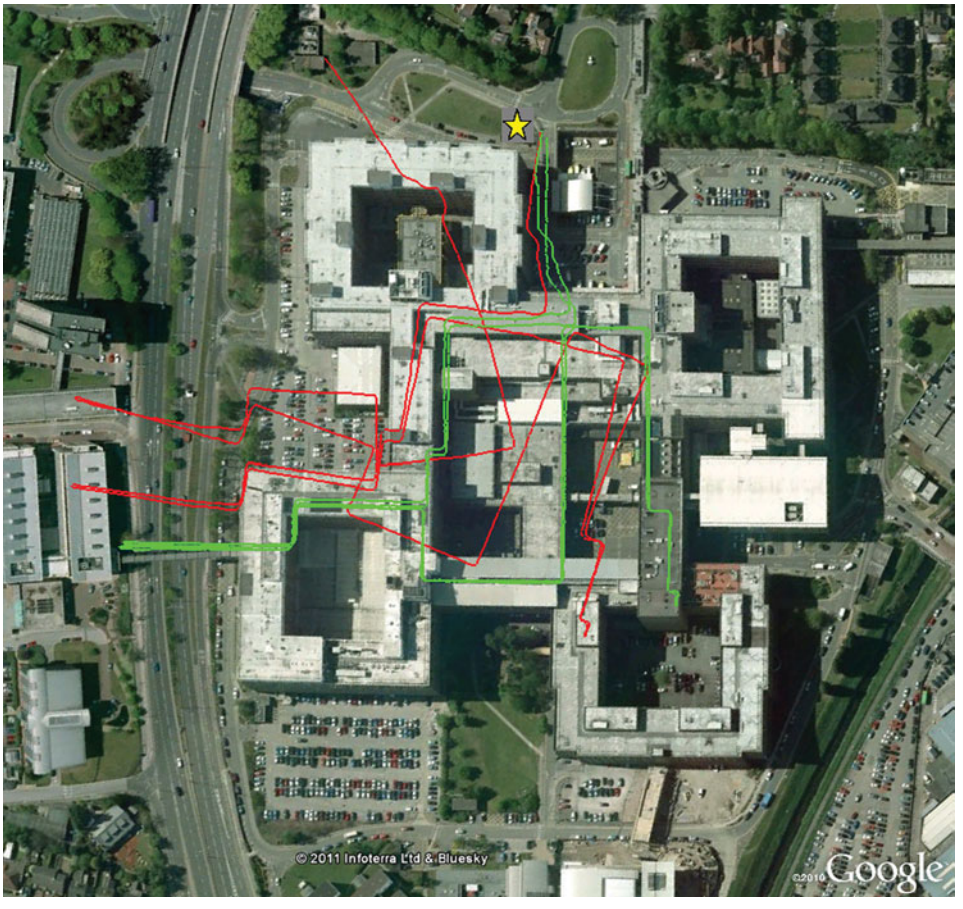

Figure 10. Example of position output from Trial 8.

6. CONCLUSIONS. This paper proposed an improved version of using 'building' heading information in the Kalman filter to restrict heading drift error.

https://doi.org/10.1017/S0373463311000518 Published online by Cambridge University Press

Previously the authors have demonstrated an effectiveness of using 'building' heading to correct heading drift for a low cost shoe mounted IMU system. It was however tested in a 2-dimensional environment excluding vertical position errors. Therefore this work extended the approach by considering a 3-dimensional situation. Furthermore this work highlights the importance of implementing the ZIHR algorithm where the user might stop walking for a long period of time, which is quite common for normal pedestrian walking. This is because a previous algorithm resulted in a significant problem with heading drift during prolonged stationary periods.

Full trials with an improved version of the algorithm were carried out in typical buildings and environments such as a car park. It was shown to give an average return position error of 4·62 m in 24 minutes of IMU-only navigation. For the vertical channel, a maximum height error of only 0·39 m was found. However, note that these figures represents the return position error (difference between start and end position), and not the accuracy of the system throughout the trial. Analysis was performed using a forward running Kalman filter only, which means that such results are achievable in real-time.

Future work will attempt to address several aspects of the system. Firstly, future work will examine the use of lower cost inertial sensors for navigation. The algorithm described is able to provide regular updates of velocity and heading which should enable the use of lower performance sensors since the errors can be continually estimated. While the sensor used in these trials is typically termed 'low cost', it is still substantially too expensive to be considered for consumer applications. Secondly, augmentation with other sensors such as GPS (when available) and magnetometers (which are typically available in low cost inertial sensor assemblies) will be explored. GPS will provide an essential source of position measurements in the environments where the signals are available and of sufficient quality to improve the position solution. The magnetometer may provide some additional measurements to correct the INS in environments where magnetic disturbances are low or buildings are not of a conventional shape. Finally, two situations have been identified where the algorithm is likely to fail: lifts and escalators. In these situations, it is likely that the zero velocity detection will provide a false positive and hence the algorithm will fail. Use of other sensors (such as a barometer), or additional measurements such as constant velocity may help to address these issues.

ACKNOWLEDGEMENTS

The authors would like to thank the Ministry of Higher Education of Malaysia and Universiti Sains Islam Malaysia (USIM) for partly sponsoring the study.

REFERENCES

Abdulrahim, K., Hide, C., Moore, T. and Hill, C. (2010). Aiding MEMS IMU with building heading for indoor pedestrian navigation. *Proceedings of Ubiquitous Positioning Indoor Navigation and Location Based Service (UPINLBS)*, 1–6. Helsinki, Finland.

Abdulrahim, K., Hide, C., Moore, T. and Hill, C. (2011). Aiding Low Cost Inertial Navigation with Building Heading for Pedestrian Navigation. *The Journal of Navigation*, **64**, 219–233.

Foxlin, E. (2005). Pedestrian Tracking with Shoe-Mounted Inertial Sensors. *Computer Graphics and Applications, IEEE*. **25**, 38–46.

Godha, S. and Lachapelle, G. (2008). Foot Mounted Inertial System for Pedestrian Navigation. *Measurement Science and Technology*, **19**, 075202.

Godha, S. (2006). Performance Evaluation of Low Cost MEMS-based IMU Integrated with GPS for Land Vehicle Navigation Application. MSc Thesis, *Department of Geomatics Engineering*. Alberta: Canada.

Hide, C., Botterill, T. and Andreotti, M. (2009). An Integrated IMU, GNSS and Image Recognition Sensor for Pedestrian Navigation. *Proceedings of International Technical Meeting of The Satellite Division of the Institute of Navigation (ION GNSS 2009)*, 527–537, Savannah, USA.

Jimenez, F. S. A. R., Prieto, C. and Guevara, J. (2009). A Comparison of Pedestrian Dead-Reckoning Algorithms using a Low-Cost MEMS IMU. *Proceedings of IEEE International symposium on Intelligent Signal Processing* Budapest, Hungary.

Lachapelle, G. (2004). GNSS Indoor Location Technologies. The International Symposium on GNSS/GPS, Sydney, Australia.

Odijk, D. and Kleijer, F. (2007). Performance of high-sensitivity GPS for personal navigation at Schiphol Airport, the Netherlands. International Global Navigation Satellite Systems Society (IGNSS) Symposium, Sydney, Australia.

Odijk, D. and Kleijer, F. (2008). Can GPS Be Used for Location Based Services at Schiphol Airport, the Netherlands?, Proceedings of the 5th Workshop on Positioning, Navigation and Communications 2008 (WPNC 08), 143–148, Hannover, Germany.

Pang, G. and Liu, H. (2001). Evaluation of a low-cost MEMS accelerometer for distance measurement. *Journal of Intelligent and Robotic Systems*, **30**, 249–265.

Park, M. and Gao, Y. (2006). Error analysis and stochastic modeling of low-cost MEMS accelerometer. *Journal of Intelligent and Robotic Systems*, **46**, 27–41.

Shin, E. H. (2005). Estimation Techniques for Low Cost Inertial Navigation. PhD Thesis, *Department of Geomatics Engineering*. Calgary: University of Calgary, 206.

Skog, I., Nilsson, J. O. and Händel, P. (2010). Evaluation of Zero-Velocity Detectors for Foot-Mounted Inertial Navigation Systems, *Proceedings of International Conference on Indoor Positioning and Indoor Navigation (IPIN 2010)*, Switzerland.